Transition probabilities for atomic hydrogen via the Migdal Effect

Ruby Unwin
Supervisor: Christopher McCabe

7CCP1500
King's College London
Faculty of Natural & Mathematical Sciences

Abstract

The Migdal effect is a phenomenon that was first discovered by Arkdady Migdal in 1939. Originally, it was assumed that once a nucleus was hit by a particle, it would recoil and the surrounding electrons would follow in it's path. Migdal, however, noticed that with a sufficient momentum transfer between the incoming particle and the nuclei, the electrons had a chance to lag behind. This would then leave the atom in an excited or ionised state.

This effect was found to be useful in experimental designs such as LUX and xenon1T, which use argon and xenon gasses in an attempt to detect dark matter with a sub-GeV mass. These experiments found that the electron emitted during the Migdal effect indeed provided an increased sensitivity and signal output relative to that of a general nuclear recoil reaction.

Now, hydrogen is being considered as a potential alternative to the previously used elements, since it is lighter and should theoretically have a greater reaction to the incoming particles. This project aims to explore whether this claim indeed holds true for hydrogen.

To do this, we will first cover the basic concepts of a hydrogen atom; its bound and unbound wave function solutions. We will then use these wave function solutions to calculate the Migdal transition probabilities for the $1s$ and $4s$ inital states. Finally, we will compare these probabilities to those obtained for argon and xenon atoms.

There will also be some computational issues encountered along the way, which will be discussed.

CONTENTS

1 INTRODUCTION

Spiral galaxies and the expansion of the universe are two of many experimental observations that give rise to the idea of there being some form of matter that we have yet to detect. The speed at which we have observed galaxies moving away from each other and the universe expanding cannot be explained by a model of physics that does not involve dark matter [1]. Indeed, computational simulations of the universe that don't take the existence of dark matter into account look very different to those that do and those simulations that take it into account in fact look remarkably similar to the universe we observe today. Despite the overwhelming support of mathematical models and astrophysical observations, dark matter has yet to be experimentally observed, nor have its properties been possible to explore. Achieving this goal of discovering and observing the properties of dark matter would be a major leap forward in many fields of physics and confirm many phenomena that are predicted by the standard model, that can only be explained by the existence of some unseen form of matter.

We know that dark matter very rarely interacts with regular matter and that when it does, these interactions are extremely weak. It also is completely unaffected by electromagnetic forces [2], which means it must be electrically neutral. This property is partly what makes detecting dark matter extremely difficult; it's hard to detect something if it doesn't interact with it's surroundings. Fortunately, dark matter does still very occasionally interact with matter, and thus there is still a chance that we can detect it with appropriate experimental setups. Such setups have to be deep underground to avoid background noise from cosmic rays, atmospheric muons and neutrinos.

There have been many proposals for what exactly dark matter could be, and each proposal has its own unique properties and methods of detecting. One such proposal is the weakly interacting massive particle, also known as WIMPs. These particles are coupled to standard model particles through weak nuclear interactions.

One possible method of detecting WIMPs is to attempt to observe them scattering with the nuclei of atoms. In these interactions, the WIMPs collide with a nucleus of mass $m_n \approx 100GeV$ and impart a momentum transfer of approximately $q_A \approx 100$MeV [4], causing the nucleus to recoil. These recoils can then be detected through ionisation, scintillation or heat production. So far, experiments using this method have been unsuccessful in detecting any WIMPs. It is believed that WIMPs may simply be lighter than originally expected, and their interactions with nuclei are simply too weak to be detected with this method.

The experiments previously described make the assumption that, when the nucleus recoils, the clouds of electrons immediately follow it. In reality, when the nucleus is struck 'suddenly', the electron clouds actually lag behind [5]. The electrons lagging behind can then excite and even ionise the atom if the momentum transfer is large enough. This effect was discovered by Arkady Migal in 1939 and is hence known as the Migdal effect [5]. For the reaction to be 'sudden' [6], the incoming particle must interact with the nucleus in such a short time span that the electron shells are unaffected, or at least so that the interaction between the particle and electrons is negligible. For this to occur, the time span of the interaction must be much shorter than the orbital period of the electrons. This condition can be tested using the following formula [7], using a neutron as an example for the incoming particle;

$$\frac{\tau_n}{\tau_e} = \left(\frac{R_0}{a_0}\right)\sqrt{\frac{m_n}{2E_n}}Z^2\alpha. \tag{1}$$

Where τ_n and τ_e are the collision timescale and electronic period respectively. In this equation, $R_0 = 1.2 \times 10^{-15}A^{\frac{1}{3}}$ [7], a_0 is the Bohr radius, m_n and E_n are the mass and energy of the incoming neutron respectfully, Z is the atomic number for the target atom, and $\alpha \approx 1/137$ is the fine structure constant.

For hydrogen ($Z = 1$, $A = 1$) interacting with a neutron with energy $E_n \approx 100keV$, we find the ratio comes to approximately 1.13×10^{-5}. We can clearly see that the collision timescale is much greater than the electronic period, and thus the reaction can be considered sudden.

For argon atoms ($Z = 18$, $A = 40$) and xenon atoms ($Z = 54$, $A = 131$) interacting with a neutron of energy 565keV, the ratio comes to be approximately 5.3×10^{-3} and 0.071 respectfully. It is not so clear here that the reaction is sudden, however it is the case that the collision timescale is still small enough for both atoms to undergo the Migdal effect reactions.

When atoms are excited or ionised through the Migdal effect, the signals of the emitted electron and x-rays are much much stronger than that of the recoiling nucleus in the previous experiments [8]. Thus, the Migdal effect has recently gained traction as a possible method of detecting low mass dark matter candidates. The effect is also easy to distinguish from other background events as it has a unique topology, shown in figure (1) [9]. When a nucleus recoils as in the Migdal effect, two distinct clusters are formed. The first cluster, Cluster A in figure (1), consists of the target atom/nuclei which is recoiling, some de-excitation electrons and the primary 'Migdal' electron which is emitted. When the atom de-excites, it emits an x-ray, which then interacts with a separate electron several cm away from the initial atom. This electron forms cluster B in figure (1).

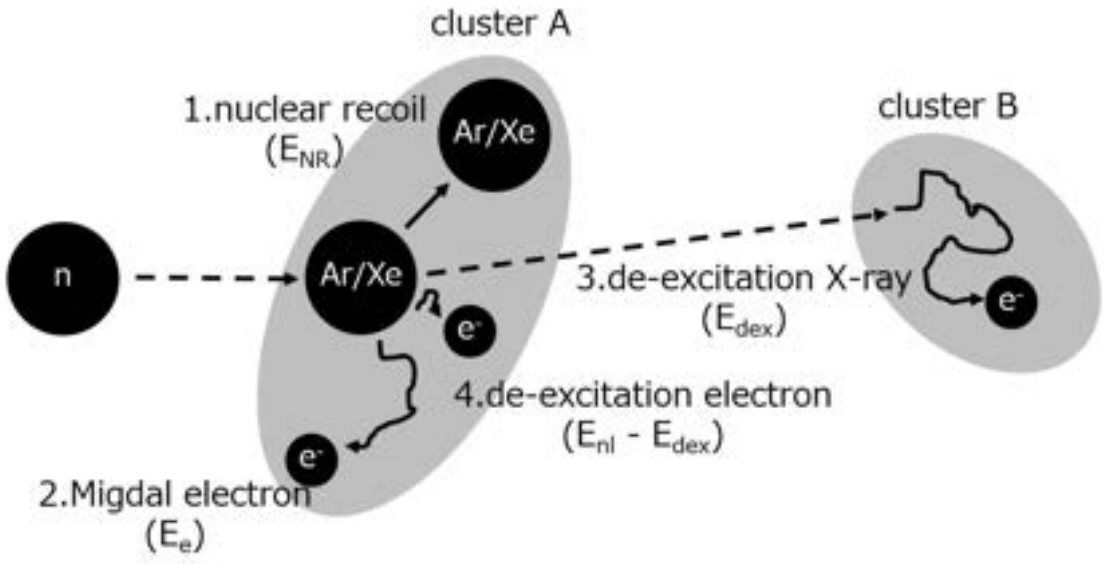

Figure 1: Topology of the Migdal Effect reaction. Cluster A holds the ionised argon/xenon atom, the Migdal electron and the de-excitation electron. Cluster B contains an electron struck by the de-excitation X-ray. [9]

The maximum energy of a standard nuclear recoil, $E_{R,max}$, and of the emitted electron, $E_{EM,max}$ are given by [10]

$$E_{R,max} = \frac{2\mu_n^2 v_{max}^2}{m_N}, \quad E_{EM,max} = \frac{\mu_n^2 v_{max}^2}{2}. \tag{2}$$

Here, $\mu_n = m_N m_{DM}/(m_N + m_{DM}$ is the dark matter-nucleus reduced mass and m_N is the mass of the target nucleus. If we take $v_{max} \approx 8 \times 10^5 \text{ms}^{-1}$ and $m_{DM} \ll m_N$, we find that indeed $E_{EM,max} \gg E_{R,max}$

Experiments such as LUX and xenon1T have been designed to make use of position sensitive detectors and tanks of argon or xenon gas to exploit the Migdal effect and increase the sensitivity of

experiments towards low mass dark matter candidates [10].

Figure (2) [8] shows the scattering rates for the Migdal effect (Dashed teal line), the Bremsstrahlung effect [**?**] (Solid blue line) and for nuclear recoil events (dash-dot pink line), taken from data obtained by LUX. Also shown is an energy cut off at 1.24keV due to the 50% efficiency of electron recoil detection [8], which imposes a lower mass limit of $0.4\text{GeV}/c^2$. It is worth noting here that the corresponding 50% efficiency for nuclear recoil detection is at 3.3keV, more than double that of the electron recoil efficiency. As seen from the graphs, for incoming dark matter particles with a mass in the range of $0.4\text{GeV}/c^2 < m_{DM} < 1\text{GeV}/c^2$, the Migdal effect has the highest rate of events for Migdal electrons with energies of $\sim 10^{-1}$keV and higher. In this mass range, the signal generated by nuclear recoils is not only much lower than both the Migdal and Bremsstrahlung effects, but also does not meet the energy threshold. Thus, the Migdal effect is clearly much more useful in the search for sub-GeV dark matter candidates than the previously used nuclear recoil approach

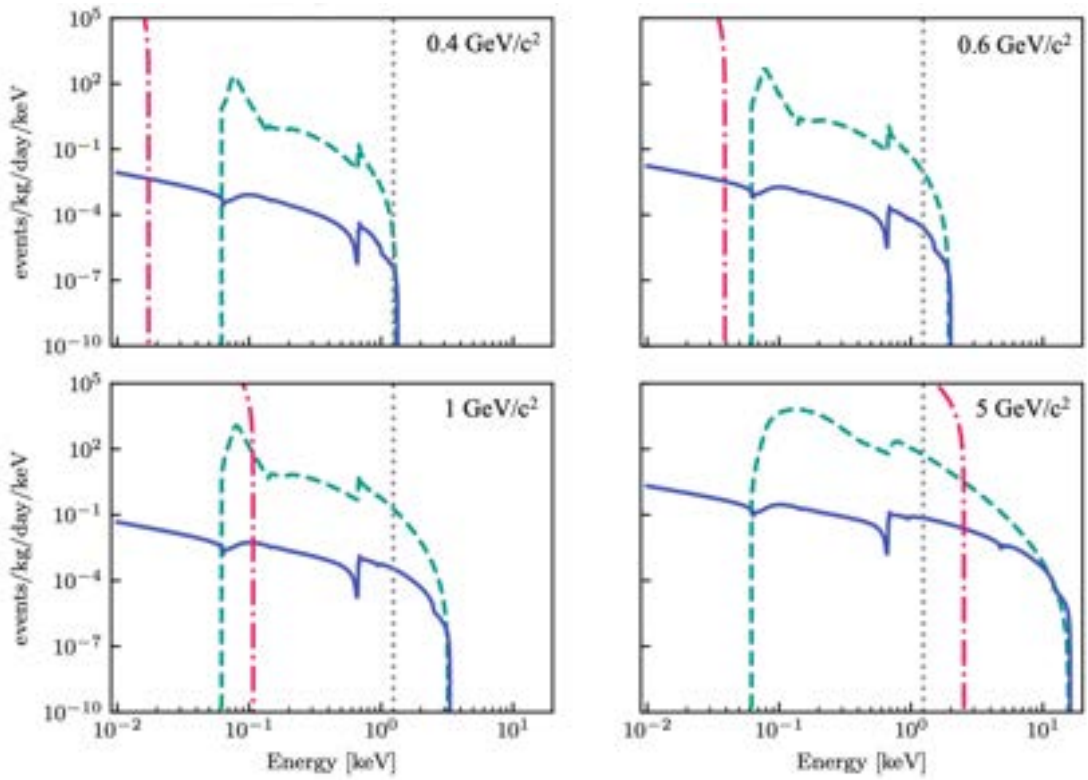

Figure 2: Scattering rates for the Migdal effect (dashed teal) Bremsstrahlung effect (solid blue) and nuclear recoil events (dash-dot pink). The dotted gray line shown is a signal cut off at 1.24 keV corresponding to the 50% efficiency of electron recoil detection . [8]

Whilst these experiments use xenon or argon in their design, hydrogen isotopes are also being considered for future experiments as hydrogen may further enhance the sensitivity of experimental designs. This project aims to theoretically evaluate the probability of excitation from the ground state for hydrogen atoms, and whether hydrogen would be a more optimal choice of target nucleus for future experimental designs.

2 THE HYDROGEN ATOM

To be able to calculate the probability of excitation for hydrogen, we first need to obtain it's wave function. A hydrogen atom consists of only an electron orbiting a single proton, and its potential energy can be found simply through Coulomb's law [12],

$$V(r) = -\frac{q_1 q_2}{4\pi\epsilon_0}\frac{1}{r} = -\frac{e^2}{4\pi\epsilon_0}\frac{1}{r}, \tag{3}$$

where $q_1 = e$ and $q_2 = -e$ are the charges of the electron and proton respectfully, and r is the displacement of the electron from the nucleus. $\epsilon_0 \approx 8.85 \times 10^{-12}$ is the permitivity of free space.

If we substitute this potential into the time independent Schrodinger's equation [13],

$$i\hbar\frac{d}{dt}\Psi = -\frac{\hbar^2}{2m}\nabla^2\Psi + V(r)\Psi, \tag{4}$$

we can solve for the the wave function of the atom, Ψ. This wave function can also be written in the form of a separation of variables; a radial variable P and a spherical harmonics variable, Y.

$$\Psi(r,\theta,\phi) = P(r)Y_\ell^m(\theta,\phi). \tag{5}$$

Through some simple manipulation, the time-independent Schrodinger's equation can then be written in the form of the 'Radial equation' [12],

$$\frac{d^2P}{dr^2} + \frac{2m}{\hbar^2}\left(E - V(r) - \frac{\ell(\ell+1)\hbar^2}{2mr^2}\right)P = 0 \tag{6}$$

.

2.1 Atomic Units

Atomic units, similarly to natural units, make it easier for us to work with certain physical systems by demanding that physical constants take the value of 1 rather than their real world values. For natural units, we set $c = \hbar = 1$. Atomic units on the other hand demand that the mass of an electron m_e, its charge e and Planck's constant $\hbar$ be set to 1. In this unit system, length is measured in terms of the Bohr radius $a_0 \approx 0.549$Å and the unit for energy is $me^4/(4\pi\epsilon_0\hbar)^2 \approx 27.2$eV [14].

This set of units is useful when working with atoms as it allows us to simplify the radial form of Schrodinger's equation by eliminating the factors of m and $\hbar$ from the equation, and simplifying $V(r)$ from $Ze^2/4\pi\epsilon_0 r$ to Z/r. The resulting equation is then [12]

$$\frac{d^2P}{dr^2} + 2\left(E + \frac{Z}{r} - \frac{\ell(\ell+1)}{2r^2}\right)P = 0, \tag{7}$$

which is much easier to solve than the original form of the equation.

2.2 Bound State

When in a bound state the electron orbiting the nucleus of an atom is confined to a discrete number of energy levels or shells, given by the principle quantum number $n = 1, 2, 3, ...$ For each shell in the atom there is also an associated energy, E_n, again defined by the principle quantum number. The electron can only have energy *exactly* equal to these values, and cannot take any value in between. The wave function for hydrogen in a bound state is then given by

$$\Psi_{n\ell m}(r,\theta,\phi) = P_{n\ell} Y_\ell^m(\theta,\phi) \tag{8}$$

where [12]

$$P_{n\ell} = \frac{1}{n(2\ell+1)!}\sqrt{\frac{Z(n+\ell)!}{(n-\ell-1)!}}\left(\frac{2Zr}{n}\right)^{\ell+1} e^{\frac{-Zr}{n}} F(-n+\ell+1, 2\ell+2, 2Zr/n) \tag{9}$$

where $\ell = 0,1,2,...,(n-1)$ and $m = -\ell,...,-1,0,1,...,\ell$ represent the angular momentum quantum number and the magnetic quantum number respectfully [15]. These quantum numbers combined with the principle quantum number define the state of an electron within the orbitals of an atom.

F is the confluent hypergeometric function, defined by the series [16]

$$F(a,b,x) = \sum_{k=0}^{\infty} \frac{(a)_k}{(b)_k k!} \tag{10}$$

$a = \frac{4\pi\epsilon_0\hbar^2}{m_e e^2}$ represents the Bohr radius, the distance from a hydrogen nucleus at which it is most likely to find an electron.

$Y_\ell^m(\theta,\phi)$ represents the spherical harmonics [17] of the atom and has well defined, tabulated values.

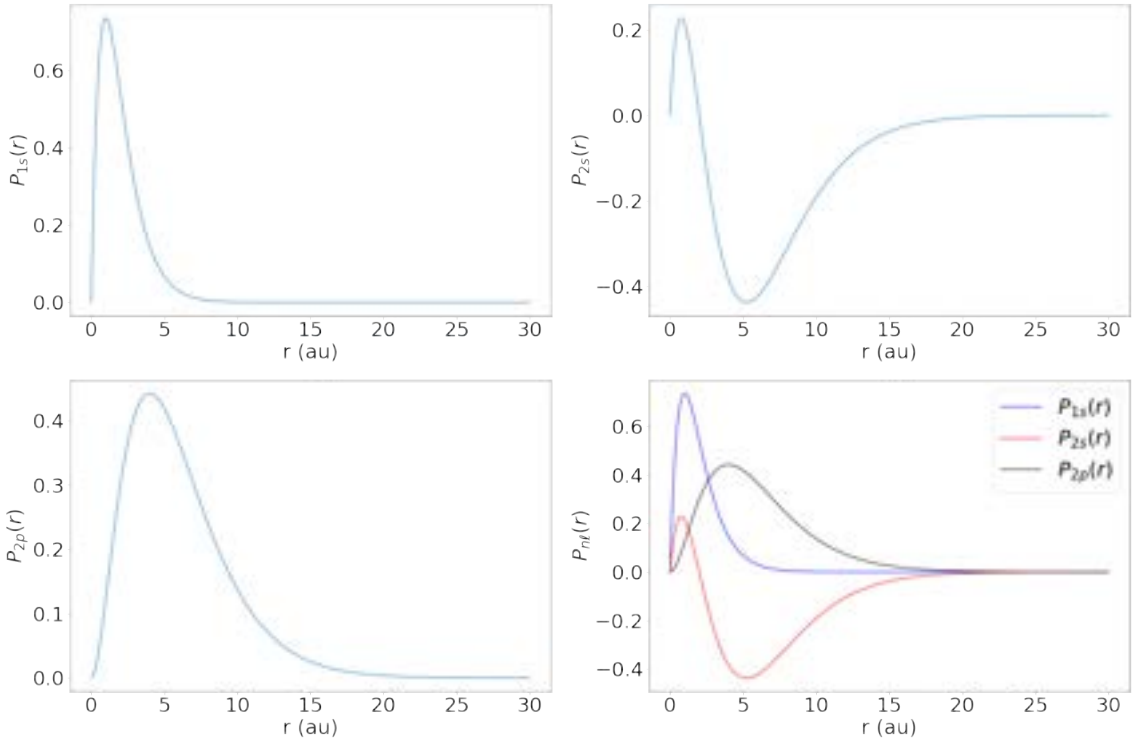

Figure 3: Plots of P_{nl} for the 1s (top left), 2s (top right) and 2p (bottom left) sub-shells in a bound hydrogen atom. The bottom right figure shows the graphs for each sub-shell combined. The distance, r, is measured in atomic units

figure (3) shows the respective plots of $P_{n\ell}(r)$ for the bound 1s, 2s and 2p orbitals, as well as a graph combining each of them.

The radial wave functions for the $1s = 10$, $2s$ and $2p$ can be respectfully expressed in the following simplified form [12]:

$$P_{10} = 2Z^{3/2} r e^{-Zr}, \tag{11}$$

$$P_{20} = \frac{1}{\sqrt{2}} Z^{3/2} r e^{-Zr/2} \left(1 - \frac{1}{2} Zr\right), \tag{12}$$

$$P_{21} = \frac{1}{2\sqrt{6}} Z^{5/2} r^2 e^{-Zr/2}. \tag{13}$$

Using these equations we can obtain the expectation values of r and r^2 ($\langle r \rangle$ and $\langle r^2 \rangle$) through simple integration;

$$\langle r \rangle_{nl} = \int_0^\infty P_{nl}^* P_{nl} r dr \quad \langle r^2 \rangle_{nl} = \int_0^\infty P_{nl}^* P_{nl} r^2 dr. \tag{14}$$

Performing these integrals for the states shown in the graphs, we find

$$\langle r \rangle_{10} = 1.5 a_0 \quad \langle r^2 \rangle_{10} = 3 a_0^2, \tag{15}$$

$$\langle r \rangle_{20} = 6 a_0 \quad \langle r^2 \rangle_{20} = 42 a_0^2, \tag{16}$$

$$\langle r \rangle_{21} = 5 a_0 \quad \langle r^2 \rangle_{21} = 30 a_0^2, \tag{17}$$

where a_o is again the Bohr radius, which is set to 1 for atomic units.

The graphs also tend to zero from around $r > 20a_0$, meaning that it is virtually impossible or at least extremely unlikely to find the electron beyond this distance from the nucleus.

Finally, we can check if the functions are orthonormal by checking the following condition:

$$\int_0^\infty P_{nl}^* P_{n'l} dr = \delta_{nn'}. \tag{18}$$

Each of the simplified radial wave functions and in fact the general function for P_{nl} indeed follow this condition, and are thus orthonormal.

2.3 Unbound States

An unbound hydrogen atom, an electron being influenced by the Coulomb potential of a proton but not bound to orbitals, also has a wave function similar to that of a bound state. However, $P_{n\ell}$ is now replaced by $P_{k\ell}$, where k is the wave number of the electron and can take continuous values [18].

$$P_{kl} = \frac{4\pi}{2k} \frac{\left|\Gamma(\ell + 1 - \frac{iZ}{k})\right| e^{\frac{\pi Z}{2k}}}{(2\ell+1)!} (2kr)^{\ell+1} e^{-ikr} F\left(\ell + 1 + \frac{iZ}{k}, 2\ell + 2, 2ikr\right). \tag{19}$$

Here, Z represents the atomic number ($Z = 1$ for hydrogen) and Γ represents the gamma function [19].

$$\Gamma(z) = \int_0^\infty x^{z-1} e^{-x} dx \tag{20}$$

This form of the wave function is also known as the Coulomb wave function [12]. Again, we can check this function for normalisation as well as for orthogonality with the unbound wave function. For the orthogonality, we can prove a similar condition as equation (18) with the bound function P_{kl} and the bound function P_{nl};

$$\int_0^\infty P_{kl}^* P_{nl} dr = 0. \tag{21}$$

This condition indeed holds true for the unbound and bound functions.

For the normality condition, however, P_{kl} does not normalise in the traditional sense and instead follows the condition

$$\int_0^\infty P_{kl}^* P_{k'l} = \frac{(2\pi)^3}{k^2}\delta(k-k'). \tag{22}$$

Figure (4) shows the plot of the unbound function $P_{0.5,0}$ in relation to r. Unlike the graphs for the bound function, this graph repeatedly oscillates. Since the function oscillates through the point $P(r) = 0$, it would be intuitive to think that at those points, the probability of finding the electron is also 0, which clearly does not make physical sense for an unbound electron. However, the graph is actually showing the wave function of a standing wave rather than a travelling wave. The travelling wave would be a linear superposition of all the standing waves, which would eliminate the 0 probability of finding an electron.

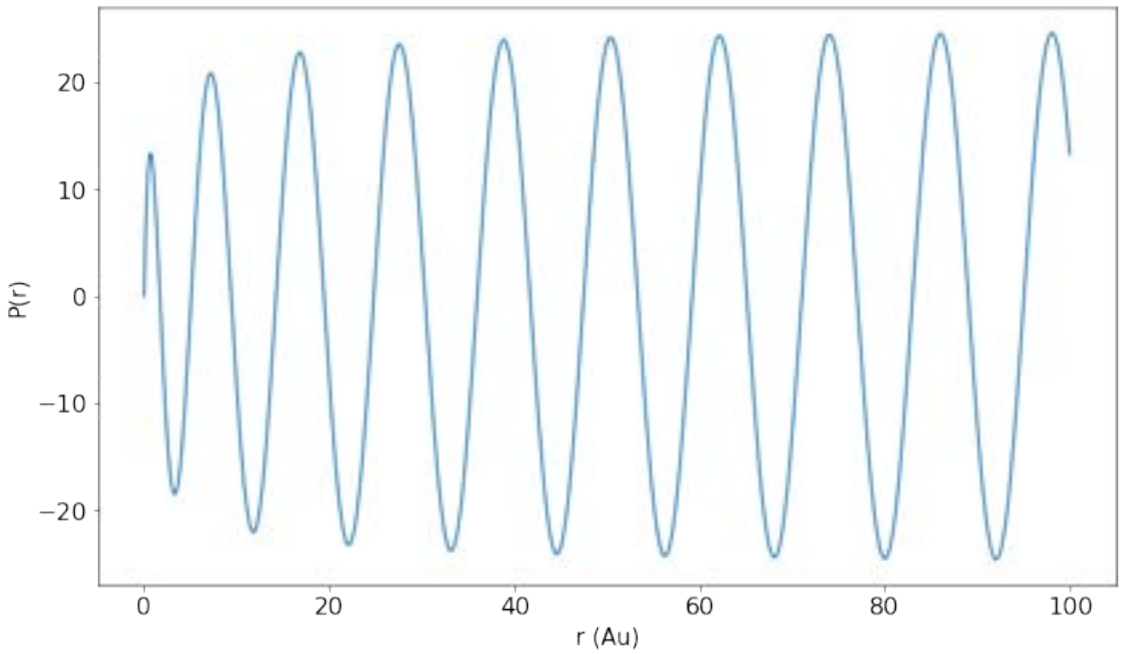

Figure 4: Plot of $P_{0.5,0}$ for the unbound Hydrogem atom

2.4 Galilean Transformation

When a system initially at rest has some velocity v or some momentum q imparted onto it, it undergoes a transformation. For non relativistic velocities ($v \ll c$), this transformation is known as a Galilean transformation.

For a hydrogen atom having some momentum imparted onto it, this transformation comes in the form of the operator [20]

$$\hat{U} = e^{iq\cdot x}. \tag{23}$$

Applying this operator to the hydrogen will then result in a new wave function, which simply describes the state of the hydrogen atom when it is in motion. This new wave function will also be a solution to the Time-independent Schrodinger equation.

2.5 hydrogen Binding Energy

The electron binding energy [22] of an atom is defined to be the minimum amount of energy required to remove an electron from a shell within the atom. This energy is always quantised, described by the electron shell n that the electron in question is occupying. In general, the binding energy for a hydrogen-like atom can be obtained from [21]

$$E_n = -\left[\frac{Z^2 m_e}{2\hbar^2}\left(\frac{e^2}{4\pi\epsilon_0}\right)^2\right]\frac{1}{n^2} \tag{24}$$

For hydrogen, $Z = 1$, and thus

$$E_n = -\left[\frac{m_e}{2\hbar^2}\left(\frac{e^2}{4\pi\epsilon_0}\right)^2\right]\frac{1}{n^2}, \tag{25}$$

Here, the negative value signifies that energy must be put into the system in order to remove the electron. This energy can also be written in the form

$$E_n = \frac{E_1}{n}, \tag{26}$$

using

$$E_1 = -\left[\frac{m_e}{2\hbar^2}\left(\frac{e^2}{4\pi\epsilon_0}\right)^2\right]\frac{1}{1^2} \approx -13.6\frac{1}{n^2}(\text{eV}). \tag{27}$$

3 The Migdal Effect

3.1 Quantum Probabilities

Now that we have obtained and explored the wave functions for both the bound and unbound states of a hydrogen atom, we can begin to calculate the probabilities for a hydrogen atom to be excited to a certain state when undergoing the Migdal effect.

Generally, the probability of a transition occurring in quantum mechanics is given by the integral

$$P(nl \to n'l') = \int \Psi^*_{n'l'm'}(x)\Psi_{nlm}(x)\,dx, \tag{28}$$

Where Ψ_{nl} and $\Psi_{n'l'}$ are the initial and final state respectfully. The asterisk denotes the complex conjugate of the function.

To calculate the probability that a hydrogen atom is excited during the Migdal effect, we essentially want to find the probability that a stationery hydrogen atom has some momentum imparted onto it,

and transitions to a new unbound state with energy E_e. Thus, from the previous discussion we should expect to find the probability in a form similar to

$$P(nl \to E_e) = \int \Psi^*_{E_e l' m'}(x) e^{iq\cdot x} \Psi_{nlm}(x) dx, \tag{29}$$

where $e^{iq\cdot x}$ is the Galilean transformation as previously discussed.

However, for continuum states, it is useful to look at the differential probability instead of the absolute probability. The differential probability is given by the following result:

$$\frac{dP(n\ell \to E_e)}{dE_e} = \sum_{\ell' m' m} \left| \int d^3x \Psi^*_{E_e \ell' m'}(x) e^{iq\cdot x} \Psi_{n\ell m}(x) \right|^2 \tag{30}$$

In this equation, E_e is the kinetic energy of the electron which is emitted as a result of the collision between the nucleus and the dark matter particle and q is the momentum which is transferred during the collision. The final result has dimensions of keV^{-1}, thus integrating over all energies will give a dimensionless quantity; the probability.

This equation can be simplified furthger to depend only on an integral over r. This can be done by exploiting the spherical symmetry of atoms and averaging over the magnetic quantum number, m, of the initial state. The differental probability then becomes

$$\frac{dP(n\ell \to E_e)}{dE_e} = \sum_{\ell' L} (2\ell+1)(2\ell'+1)(2L+1) \left[\begin{pmatrix} \ell & \ell' & L \\ 0 & 0 & 0 \end{pmatrix} \right]^2 \cdot \frac{k}{4\pi^2} \cdot \left| \int dr P_{E_e \ell'}(r) P_{n\ell}(r) j_L(qr) \right|. \tag{31}$$

Where $P_{E_e \ell'}$ and $P_{n\ell}$ are the Coulomb and bound wave functions respectfully, L is the total angular momentum of the system. We have also introduced two new functions, the spherical bessel function of the first kind $j_L(qr)$ and the Wigner 3-j symbol, which is the term that resembles a matrix.

3.2 Spherical Bessel function of the First Kind

The spherical bessel function, $j_\nu(z)$ is defined by [23]

$$j_\nu(z) \equiv \sqrt{\frac{\pi}{2z}} J_{\nu+1/2}(z), \tag{32}$$

where $J_{\nu+1/2}(z)$ is a Bessel Function of the First kind, defined by

$$j_\nu(z) = \frac{1}{2\pi i} \oint e^{(z/2)(t-1/t)} t^{-\nu-1} dt. \tag{33}$$

Of course, in our equation for the differential probability we have $\nu = L$ and $z = qr$.

Figure (5) shows the graphs for the first six spherical bessel functions, from $j_0(z)$ to $j_5(z)$.

3.3 Wigner 3-j Symbol

The wigner 3-j symbol is usually expressed in the form [24]

$$\begin{pmatrix} l_a & l & l_b \\ m_1 & m_2 & m_3 \end{pmatrix}. \tag{34}$$

However in our case, each of m_1, m_2 and m_3 are set to zero. l_a, l and l_b are then clearly ℓ, ℓ' and L respectfully. The values of the Wigner-3j symbol are shown in figure (6), where

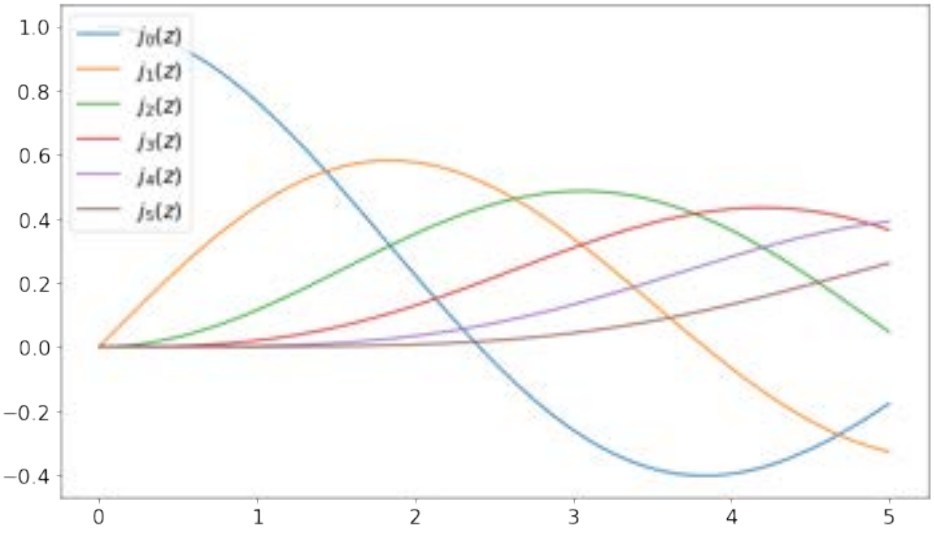

Figure 5: The first six Spherical Bessel functions of the first kind, from $j_0(z)$ to $j_5(z)$

$$\Lambda_{l_a l l_b} = \frac{1}{2}\begin{pmatrix} \ell & \ell' & L \\ 0 & 0 & 0 \end{pmatrix}^2. \tag{35}$$

l_a	l	l_b	$\Lambda_{l_a l l_b}$	l_a	l	l_b	$\Lambda_{l_a l l_b}$	l_a	l	l_b	$\Lambda_{l_a l l_b}$
0	0	0	1/2	2	0	2	1/10	3	1	4	2/63
0	1	1	1/6	2	2	2	1/35	3	3	4	1/77
0	2	2	1/10	2	4	2	1/35	3	5	4	10/1001
0	3	3	1/14	2	1	3	3/70	3	7	4	35/2574
0	4	4	1/18	2	3	3	2/105				
				2	5	3	5/231	4	0	4	1/18
1	0	1	1/6	2	2	4	1/35	4	2	4	10/693
1	2	1	1/15	2	4	4	10/693	4	4	4	9/1001
1	1	2	1/15	2	6	4	5/286	4	6	4	10/1287
1	3	2	3/70					4	8	4	245/21879
1	2	3	3/70	3	0	3	1/14				
1	4	3	2/63	3	2	3	2/105				
1	3	4	2/63	3	4	3	1/77				
1	5	4	5/198	3	6	3	50/300				

Figure 6: Table of values for the Wigner-3j symbol, with various combinations of l_a, l and l_b

3.4 Units conversion

Finally, the current form of the differential probability we have is in terms of natural units. In atomic units, the radial wave functions are

$$P_{1s}(R) = 2Re^{-R}, \tag{36}$$

$$P_{K\ell'}(R) = \frac{4\pi}{2K} \frac{\left|\Gamma(\ell+1-\frac{iZ}{K})\right| e^{\frac{\pi Z}{2K}}}{(2\ell+1)!} (2KR)^{\ell+1} e^{-iKR} F\left(\ell+1+\frac{iZ}{K}, 2\ell+2, 2iKR\right) \tag{37}$$

and the differential probability becomes

$$\frac{dP(n\ell \to E_e)}{dE_e} = (m_e a_0)^2 \sum_{\ell' L} (2\ell+1)(2\ell'+1)(2L+1) \left[\begin{pmatrix} \ell & \ell' & L \\ 0 & 0 & 0 \end{pmatrix}\right]^2 \cdot \frac{K}{4\pi^2} \cdot \left| \int dr P_{K\ell'}(R) P_{n\ell}(R) j_L(QR) \right|. \tag{38}$$

To make these conversions, we have used Q(a.u) = q(keV)a_0, where $a_0 = (m_e\alpha)^{-1} = 1/3.7289395\text{keV}^{-1}$, E(a.u) = E(eV)/E_H where $E_H = m_e\alpha^2 \approx 27.21138625$eV and K(a.u) = $\sqrt{2\text{E(a.u)}}$. Finally, the .factor of $(m_e a_0)^2$ is to ensure that the final result is in units of keV^{-1}.

3.5 Migdal Transition Probabilities

Finally, to calculate the probability that a hydrogen atom is ionised from the initial state Ψ_{nl} to a final state where the electron has kinetic energy E_e, we simply integrate the differential probability over all E_e.

$$P(nl \to E_e) = \int_0^\infty \frac{dP(n\ell \to E_e)}{dE_e} dE_e \tag{39}$$

4 Results

Unfortunately, the python code written throughout this project was unsuccessful in providing realistic probabilities for the ionisation of different states of a hydrogen atom.

We can tell this is the case as, when calculating the probability for starting states of $n \geq 4$, the result is a probability of 182%. This is clearly physically impossible, and thus there must be a fault in the code.

There are a few possible sources for this error. The first source is python's integration routine, as it is hard to determine whether the routine is correctly reading the function and/or integrating it in respect to E or some other term.

Secondly, the interpolation of the function may be faulty, causing the function to cross the x and y axis where it shouldn't; dP/dE_e should tend to infinity as $E_e \to 0$ and should tend to zero as $E_e \to \infty$. However, the interpolation is most likely extending the function incorrectly and extrapolating far beyond the axis, which in turn causes the integration to be incorrect and return negative values.

Finally, and also partially as a result of the interpolation issue, it is difficult to determine which values should be used as accurate bounds for the integral and thus hard to accurately determine the integral itself. If the bound is chosen to be too high, the interpolation will be less accurate and could effect the final result, some times returning negative values of probability. If the chosen bound is too small, then it can not be used as an appropriate approximation of an integral from 0 to ∞.

4.1 Expected results

Fortunately, these transitional probabilities have previously been calculated in other papers [25] and we can use these as an example of what we should expect.

In the paper, we have tables for the transition probabilities of various initial states $(n_0 l_0)$ and values of q. It is worth noting that the paper has used the notation of p, which in our case is exactly identical to q.

In figure (7) [25], the initial state being tested is $nl = 10$, i.e the ground state of hydrogen. The value of q has then been set to 0.15. The ionisation probability obtained from these conditions is 0.76% [25]. The table also shows the probability of transitioning from the ground state (10) to various other bound states given by the values of (nl) in the table.

n \ l	0	1	2	3	$\sum_l$
1	97.78				97.78
2	0.01	1.18			1.19
3	0.00	0.20	0.00		0.20
4	0.00	0.07	0.00	0.0000	0.07

Figure 7: Table of values for the probability of excitation of hydrogen from the ground state (Ψ_{10}) to the state described by nl. in the rightmost column is the sum over l of all the probabilities for that sub-shell. $q = 0.15$

figure (8) [25] shows the results similar to figure (7), now using a value of $q = 1$ instead of $q = 0.15$. With this higher value of q, the probability of ionisation has jumped many fold up to 44.7% [25], over fifty times the original probability.

n \ l	0	1	2	3	4	5	6	7	8	$\sum_l$
1	41.0									41.0
2	2.72	6.11								8.82
3	0.68	1.81	0.19							2.68
4	0.27	0.76	0.10	0.00						1.13
5	0.13	0.38	0.06	0.00	0.00					0.58
6	0.08	0.22	0.04	0.00	0.00	0.00				0.33
7	0.05	0.14	0.02	0.00	0.00	0.00	0.00			0.21
8	0.03	0.09	0.02	0.00	0.00	0.00	0.00	0.00		0.14
9	0.02	0.07	0.01	0.00	0.00	0.00	0.00	0.00	0.00	0.10

Figure 8: Table of values for the probability of excitation of hydrogen from the ground state (Ψ_{10}) to the state described by nl. in the rightmost column is the sum over l of all the probabilities for that sub-shell. $q = 1$

We can already gain some information on the nature of hydrogen from these two tables. First, we can see that as q increases, the probability for the atom to be ionised and/or transition also increases greatly. This is to be expected as an increase in q means the hydrogen nucleus is having more momentum imparted onto it during the reaction, and thus will experience a greater recoil. Since

the nucleus experiences a greater recoil, the electron clouds are also much more likely to lag behind.

Secondly, we can see that the probability of a transition decreases with the values of n and l for the state which we are calculating the probability for. This is once again expected as the effect of the nuclear recoil and the energy that the electrons gain must be much greater to reach the shells that are further away from the nucleus. The highest of these probabilities of course being the "transition" from (10) to (10), since this is the same as saying the probability of the hydrogen atom staying in its original state.

We can then move on to exploring what happens when we start with a different initial state, as in figures (9) and (10) [25].

Figure (9) [25] once again shows the % probabilities of a transition from an initial state to a final state, with $q = 0.15$. However, this time the initial state is $(nl) = (40)$ rather than $(nl) = (10)$. Under these conditions, it was found that there is a 9.22% chance of ionisation [25].

n \ l	0	1	2	3	4	5	6	7	$\sum_l$
1	0.0								0.0
2	0.1	0.0							0.2
3	4.1	0.7	0.0						4.9
4	0.0	8.0	19.8	7.9					35.6
5	1.1	4.2	0.2	11.9	10.1				27.6
6	1.0	0.9	1.5	3.5	0.1	3.6			10.6
7	0.6	0.2	1.3	0.9	0.5	0.6	0.6		4.7
8	0.4	0.0	0.9	0.3	0.4	0.1	0.3	0.1	2.4
9	0.3	0.0	0.6	0.1	0.3	0.0	0.1	0.0	1.5
10	0.2	0.0	0.4	0.0	0.2	0.0	0.1	0.0	0.9
11	0.1	0.0	0.3	0.0	0.1	0.0	0.0	0.0	0.6
12	0.1	0.0	0.2	0.0	0.1	0.0	0.0	0.0	0.5
13	0.1	0.0	0.2	0.0	0.1	0.0	0.0	0.0	0.3
14	0.1	0.0	0.1	0.0	0.1	0.0	0.0	0.0	0.3

Figure 9: Table of values for the probability of excitation of hydrogen from the ground state (Ψ_{40}) to the state described by nl. in the rightmost column is the sum over l of all the probabilities for that sub-shell. $q = 0.15$

Figure (10) shows a similar situation to figure (9), but this time setting $q = 0.3$. here, the probability for ionisation is 74.0% [25].

Interestingly, we can see in these tables that there is a non-zero chance of the hydrogen atom being in a lower quantum state than it begins in, in fact in figure (10) we see there is actually most likely to transition to a lower state. For the circumstances in figure (9), there is a negligible chance of the atom remaining in its original state.

The probability to become ionised under the circumstances used in figure (9) is much higher than in figure (7). This is to be expected since the electrons in outer shells of an atom (in this case, the 4th shell) have a much weaker attraction to the nucleus. This can be inferred from the inverse relation between potential energy and displacement in Coulomb's law, equation (3).

Finally, whilst every other setup of variables resulted in only one peak in the probability, figure (10) instead has two peaks; one at $n = 3$ and another at $n = 7$.

n \ l	0	1	2	3	4	5	6	7	8	9	$\sum_l$
1	0										0
2	0.96	0.05									1.01
3	0.16	3.50	3.15								6.81
4	0.44	0.17	0.57	0.34							1.52
5	0.13	0.01	0.07	0.04	0.88						1.13
6	0.03	0.02	0	0	0.94	1.13					2.13
7	0	0.01	0.02	0	0.59	1.25	0.35				2.23
8	0	0	0.03	0.02	0.35	1.02	0.47	0.05			1.94
9	0	0	0.03	0.03	0.21	0.78	0.46	0.08	0		1.59
10	0	0	0.02	0.03	0.13	0.59	0.41	0.10	0	0	1.28

Figure 10: Table of values for the probability of excitation of hydrogen from the ground state (Ψ_{40}) to the state described by nl. in the rightmost column is the sum over l of all the probabilities for that sub-shell. $q = 0.3$

4.2 Obtained results

The code that was written was designed to take input values for Q, n and l, and output both a graph of the differential probability against E_e as well as the integrated ionisation probability for the given initial state (nl).

Running the python script with an initial state (nl) = 10 and summing l' and L from 0 to 5 results in a probability of ionisation of 0.389%, which is not too far from the expected result for this initial state obtained in figure (7). The graph obtained from this initial state is shown in figure (11).

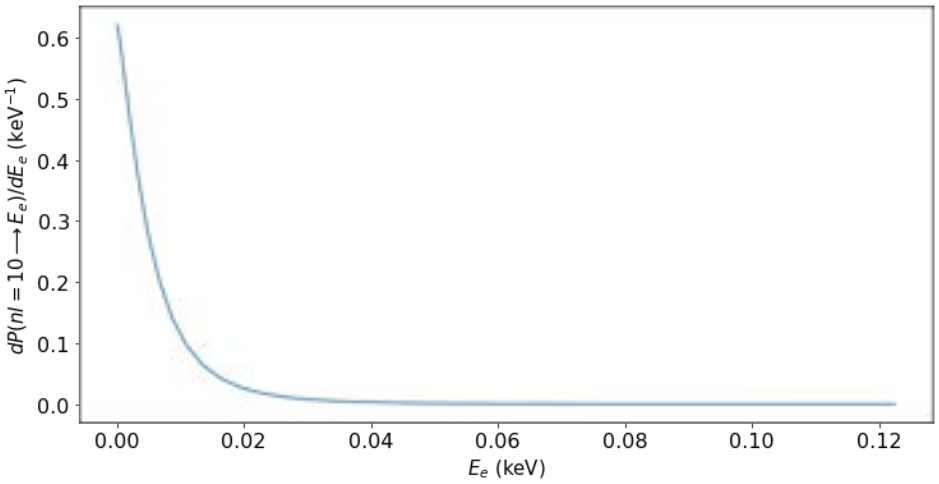

Figure 11: Graph of dP/dE_E against E_e, with the ground state as the initial state. $q = 0.15$

Starting with an initial state (nl) = 40, however, the probability now comes out to be 68.4%. This is not immediately problematic, as it is under 100%, however the value is now much much higher than the expected value from figure (9). The graph for this initial state is shown in figure (12). Whilst figure (11) seemed to have reasonable values on the y-axis, figure (12) has a y-axis going up to and beyond 2000keV^{-1}, which is alarming for a probability distribution. Once integrated, however, this value does still seem to come back down to a physically possible probability.

The issues begin arising when we alter the value of q. Going again back to the initial state (nl) = 10.

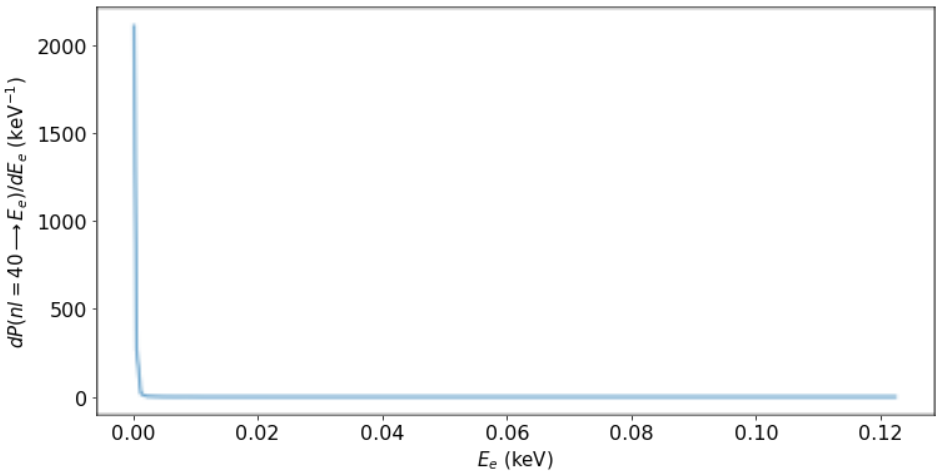

Figure 12: Graph of dP/dE_E against E_e, with the state Ψ_{40} as the initial state. $q = 0.15$

but using the $q = 1$. We now find that the probability is 233.5%, which is clearly physically impossible. Interestingly the graph produced for this value of q (figure (13)) actually looks very reasonable and resembles a typical probability distribution, including a local maximum.

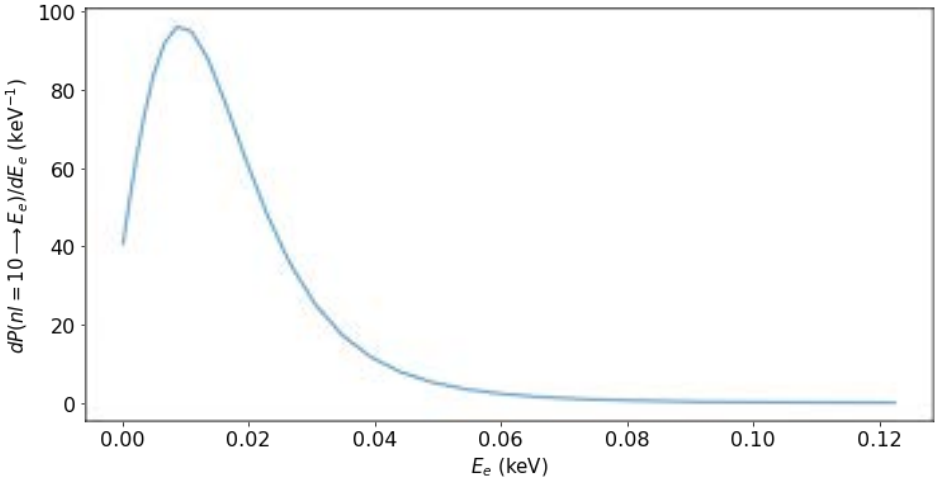

Figure 13: Graph of dP/dE_E against E_e, with the ground state as the initial state. $q = 1$

Finally, if we again look at the $(nl) = 40$ state with $q = 0.3$, we now find the probability to be 1096%. Again this is clearly physically impossible, and the graph obtained (figure (14)) no longer looks reasonable.

5 RESULTS IN CONTEXT

5.1 argon transition probability

By themselves, these results do not provide any insight into the goal of this project; to find whether or not hydrogen is a $better$ choice than argon or xenon for dark matter detection experiments. Thus,

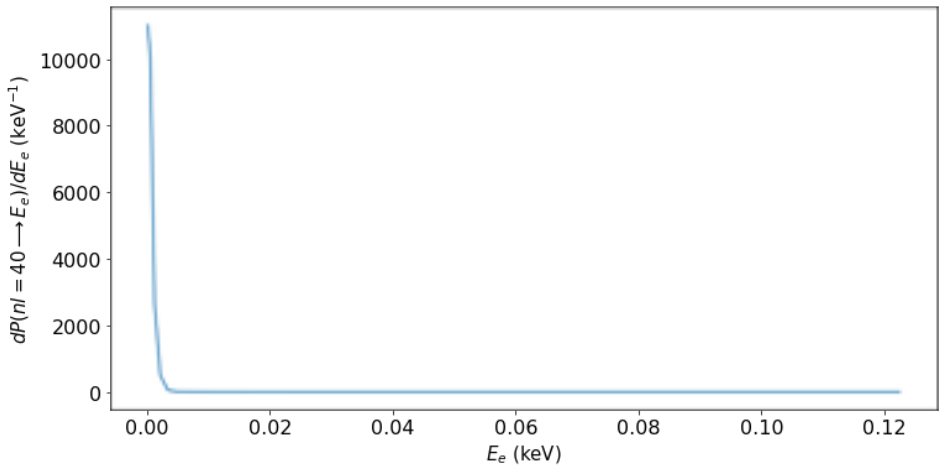

Figure 14: Graph of dP/dE_E against E_e, with the state Ψ_{40} as the initial state. $q = 0.3$

we must compare these results to those obtained for argon and xenon atoms. We can find take these results from a paper that has similarly managed to calculate the transition probabilities for each element [4].

We will first look at the transition probabilities for argon. For the following tables, a q value of $q = m_e \times 10^-3$ [4] has been used, where m_e is the mass of an electron. This value is in terms of natural units, and converts to approximately $q = 0.137$. This is not the exact value used for the hydrogen transition probabilities but should be close enough to allow us to compare results.

Figure (15) [4] shows the probabilities for an argon atom to transition from different initial states described by (n, l) to a final state, as well as the total ionisation probability in the rightmost column. Also shown are the binding energies, E_{nl} of the respective orbitals. All omitted probabilities are either forbidden or of negligible magnitude.

Ar ($q_e = m_e \times 10^{-3}$)

(n,ℓ)	$\mathcal{P}_{\to 3d}$	$\mathcal{P}_{\to 4s}$	$\mathcal{P}_{\to 4p}$	$\mathcal{P}_{\to 4d}$	$\mathcal{P}_{\to 5s}$	$\mathcal{P}_{\to 5p}$	E_{nl} [eV]	$\frac{1}{2\pi}\int dE_e \frac{dp^+}{dE_e}$
$1s$	–	–	1.3×10^{-7}	–	–	4.3×10^{-8}	3.2×10^{3}	7.3×10^{-5}
$2s$	–	–	5.3×10^{-6}	–	–	1.8×10^{-6}	3.0×10^{2}	5.3×10^{-4}
$2p$	4.3×10^{-6}	5.0×10^{-6}	–	3.0×10^{-6}	1.3×10^{-6}	–	2.4×10^{2}	4.6×10^{-3}
$3s$	–	–	5.3×10^{-7}	–	–	1.1×10^{-6}	2.7×10	1.4×10^{-3}
$3p$	7.9×10^{-3}	8.5×10^{-3}	–	4.0×10^{-3}	1.2×10^{-3}	–	1.3×10	6.4×10^{-2}

(n,ℓ)	$3d$	$4s$	$4p$	$4d$	$5s$	$5p$
E_{nl}[eV]	1.6	3.7	2.5	0.88	1.6	1.2

Figure 15: Table of Migdal transition probabilities for an argon atom, with $q \approx 0.137$, starting at an initial state $\Psi_{n,l}$. The two right-most columns show the ionisation energy of the atom and the integrated probability of ionisation respectfully.

5.2 xenon transition probability

Figure (16) [4] again shows a similar table to (15) but for xenon atoms rather than argon.

Xe ($q_e = m_e \times 10^{-3}$)

(n,ℓ)	$\mathcal{P}_{\to 4f}$	$\mathcal{P}_{\to 5d}$	$\mathcal{P}_{\to 6s}$	$\mathcal{P}_{\to 6p}$	$E_{n\ell}$ [eV]	$\frac{1}{2\pi}\int dE_e \frac{dp^c}{dE_e}$
1s	–	–	–	7.3×10^{-10}	3.5×10^{4}	4.9×10^{-6}
2s	–	–	–	1.8×10^{-8}	5.4×10^{3}	3.0×10^{-5}
2p	–	3.0×10^{-8}	6.5×10^{-9}	–	4.9×10^{3}	1.3×10^{-4}
3s	–	–	–	2.7×10^{-7}	1.1×10^{3}	1.1×10^{-4}
3p	–	3.4×10^{-7}	4.0×10^{-7}	–	9.3×10^{2}	6.0×10^{-4}
3d	2.3×10^{-9}	–	–	4.3×10^{-7}	6.6×10^{2}	3.6×10^{-3}
4s	–	–	–	3.1×10^{-6}	2.0×10^{2}	3.6×10^{-4}
4p	–	4.1×10^{-8}	3.0×10^{-5}	–	1.4×10^{2}	1.5×10^{-3}
4d	7.0×10^{-7}	–	–	1.5×10^{-4}	6.1×10	3.6×10^{-2}
5s	–	–	–	1.2×10^{-4}	2.1×10	4.7×10^{-4}
5p	–	3.6×10^{-2}	2.1×10^{-2}	–	9.8	7.8×10^{-2}

(n,ℓ)	$4f$	$5d$	$6s$	$6p$
$E_{n\ell}$[eV]	0.85	1.6	3.3	2.2

Figure 16: Table of Migdal transition probabilities for a xenon atom, with $q \approx 0.137$, starting at an initial state $\Psi_{n,l}$. The two right-most columns show the ionisation energy of the atom and the integrated probability of ionisation respectfully.

5.3 Discussion of results

Before comparing the values from the tables, we should first note that the tables of values for hydrogen had summed over all values of l for the ionisation probability. Thus we will also sum over the values obtained for the ionisation energy and probabilities for the argon and xenon results.

Comparing the values from figures (15) and (16), we can first see that the energy required to ionise each atom is magnitudes greater than that for hydrogen. Reading off the tables, we see that for the $n = 1$ sub-shell, argon has an ionisation energy of $E_n = 3.2 \times 10^3$eV and xenon has an ionisation energy of $E_n = 3.5 \times 10^4$eV. We already know from the previous sections that the ionisation energy of hydrogen in this state is $E_n = 13.6$eV, which is approximately 235 times lower than the ionisation energy for argon and an even greater 2500 times lower than that of xenon. Thus, hydrogen is already clearly much more likely to be ionised than either argon or xenon, but we can look at the shells further out to make it even clearer. Indeed argon only achieves an ionisation energy on the same order of magnitude as hydrogen's ground state ionisation energy when the electron is in the $n = 3$ sub-shell, where the ionisation energy is $E_n = 41.6$eV. The ionisation energy of hydrogen at this shell is then $E_n = 13.6/3^2$eV,

which is approximately 1.51eV, still much lower than argon's ionisation energy. Similarly for xenon, it isn't until we look at the $n = 5$ sub-shell that the ionisation energy beings to look similar to that of the ground state ionisation energy for hydrogen, $E_n = 32.4$eV. Comparing this to the corresponding ionisation energy for hydrogen, we find $E_n = 13.6/5^2 = 0.544$eV, much lower than the ionisation energy at this shell for xenon.

Next, we can look at the actual probabilities for the atoms to be ionised or excited. Since the paper used a value of $q \approx 0.137$, we will only compare the values obtained to those of the tables using $q = 0.15$. Starting with the ground state of hydrogen, we found that the probability of ionisation was 0.76%. Looking at the tables for argon, we see that the integrated ionisation probability of ionisation from the $(1s)$ state is 0.0073%. The ionisation probability for hydrogen is thus approximately one-hundred times greater when the initial state is at this orbital. Similarly for xenon, the probability is 0.00049%, 1500 times smaller than the hydrogen probability.

For the excitation probabilities, for example, we found that hydrogen had a 0.07% chance to be excited to the $n = 4$ state (where the probabilities for $nl = 40$, $nl = 42$ and $nl = 43$ were negligible). The corresponding probability for argon is then 1.3×10^{-5}%, which clearly shows this transition is much more unlikely in the argon atom. In the data for xenon, this transition probability was negligible and thus omitted entirely.

Now we can look at the ionisation probabilities when starting with a different initial state, $(nl) = (40)$. For this state, hydrogen was to found to have a 9.22% chance of being left ionised during the Migdal reaction. Summing over all ionisation probabilities across the orbitals for xenon, the probability is found to be only 3.786%, once again a smaller chance than for hydrogen.

Finally, we can look at the excitation probabilities for the initial state $(nl) = (40)$. Unfortunately, figure (15) does not have the data for this initial state, and thus we can only look at the probabilities for xenon atoms. For this initial state, we found that hydrogen has a 10.6% chance to transition to the $n = 6$ shell. For xenon, the corresponding probability is found to be 0.01831, which is again much lower than the value obtained for hydrogen.

From these comparisons we see that, when looking at the ground state of an atom, hydrogen is far more likely to transition to a higher state or be left ionised by a collision with a neutron (or potential dark matter particle) than both an argon and xenon atom. In comparison, the electrons in a hydrogen atom also require a far smaller energy input to be stripped from their shells and leave the Coulomb potential of the nucleus. This would seem to indicate that hydrogen would in fact be a better candidate for a target particle than an argon or xenon atom, since it is far more easily ionised and should theoretically produce a higher rate of events. It should also be more easily ionised by particles of lower mass than xenon, which would potentially allow for experiments such as LUX and xenon1T to detect dark matter candidates with masses lower than that of the 0.4GeV lower bound that was previously found.

It may also be worth noting that when calculating the ratio between the collision and electronic timescales, the hydrogen atom conformed to the condition τ_n/τ_e much more strongly than the ratio for both argon and xenon atoms. This is mostly to be expected as the hydrogen atom only has one electron rather than multiple shells filled with electrons, which in the case of argon and xenon make it much harder for an incoming particle to strike the nucleus without affecting the orbits of said electrons. It could also then be said that the probability of the Migdal effect occuring at all within the hydrogen atom should be higher than in argon or xenon.

6 CONCLUSION

In conclusion, we have covered the basics of the motivation behind exploring and testing the limits of the Migdal effect. Primarily, the Migdal effect is currently being explored as a potential method of detecting dark matter candidates such as WIMP's with a mass below 1GeV. Previous experiments have successfully shown that by detecting the Migdal effect occurring during the collision between a particle and the nucleus of an argon or xenon atom, it is possible to detect much smaller particles than when attempting to detect only basic nuclear recoil reactions. Research is now being done to find alternative targets to argon or xenon which may further enhance the sensitivity of such experimental setups.

One such alternative is hydrogen (and it's isotopes). hydrogen is a much lighter element than both of argon and xenon and thus should have a more significant reaction to being struck by an incoming particle, and thus should allow for the detection of particles with even lower mass. Indeed, we have managed to find the probability of certain excitations or ionisations within the hydrogen atom, and shown that they far exceed the probability of the same event occuring within an argon or xenon atom. Thus shown that a hydrogen atom should make a more suitable target in future experimental designs.

There are, however, two avenues that have yet to been explored in this project. The first of which is that we have not yet found the probability for Migdal transitions within hydrogen isotopes such as deuterium and tritium. It can however be predicted that similar results will be achieved showing that deuterium and perhaps tritium may still provide a more suitable experimental target. These predictions should still be explored however, as the difference in mass between hydrogen and tritium may mean tritium is not as suitable of a replacement.

Secondly, hydrogen can not be used in these experiments (or rather, it would be extremely difficult to) since it is very rare and difficult to maintain hydrogen in its atomic form. For this reason hydrocarbon gasses containing hydrogen in their chemical structure, such as methane, are being considered as a possible replacement to argon and xenon. Since the hydrogen in methane is of course bonded to carbon atoms, the ways in which it will interact and respond to an incoming particle could be negligibly different to the theoretical values obtained for atomic hydrogen, or it could be of enough significance to mean hydrogen is not at all a suitible replacement for argon and xenon. These differences and theoretical probabilities should thus also be explored in order to determine if methane can be used to produce experimental designs with higher sensitivities.

REFERENCES

[1] N. A. Bahcall. *"Dark matter universe"*. doi:10.1073/pnas.1516944112

[2] CERN. *"Dark matter"*. https://home.cern/science/physics/dark-matter.

[3] Britannica, T. Editors of Encyclopaedia. *"weakly interacting massive particle."* Encyclopedia Britannica, August 1, 2018. https://www.britannica.com/science/weakly-interacting-massive-particle.

[4] M. Ibe, W. Nakano, Y. Shoji, K. Suzuki. *"Migdal Effect in dark matter direct detection experiments"* JHEP, March 30, 2018. arXiv:1707.07258 .

[5] A. B. Migdal. *"Qualitative Methods In Quantum Theory"*, 1977. doi:10.1201/9780429497940.

[6] J. D. Talman, A. M. Frolov. *"Excitations of light atoms during nuclear reactions with fast neutrons"* Physics Review A, March 23, 2006. doi:10.1103/PhysRevA.73.032722.

[7] R. Unwin. *"The Migdal Effect"*, 2022.

[8] D. S. Akerib, S. Alsum, H.m Araújo, X. Bai, *"Results of a Search for Sub-GeV Dark Matter Using 2013 LUX Data"*, Phys. Rev. Lett. 122, October 5, 2019. doi:10.48550/arXiv.1811.11241.

[9] K. D. Nakamura, K. Miuchi, S. Kazama, Y. Shoji, M. Ibe, W. Nakan. *"Detection capability of Migdal effect for argon and xenon nuclei with position sensitive gaseous detectors"* PTEP, September 13, 2020. doi:10.1093/ptep/ptaa162.

[10] M. J. Dolan, F. Kahlhoefer, C. McCabe. *"Directly detecting sub-GeV dark matter with electrons from nuclear scattering"* August 22, 2018. doi:10.48550/arXiv.1711.09906.

[11] Britannica, T. Editors of Encyclopaedia. *"bremsstrahlung."* Encyclopedia Britannica, September 25, 2018. https://www.britannica.com/science/bremsstrahlung.

[12] W. R. Johnson. *"Lectures on Atomic Physics"* January 4, 2016. https://www3.nd.edu/ johnson/Publications/book.pdf.

[13] C. R. Nave. *"Schrodinger Equation"* Hyperphysics (accessed on April 20, 2022). http://hyperphysics.phy-astr.gsu.edu/hbase/quantum/Scheq.html.

[14] Anon. *"Atomic and Molecular Calculations Are Expressed in Atomic Units."* March 18, 2020. https://chem.libretexts.org/@go/page/210838.

[15] Anon. "Quantum Numbers for Atoms." January 17, 2021. https://chem.libretexts.org/@go/page/1709.

[16] E. W. Weisstein. *"Confluent Hypergeometric Function of the first kind."* Mathworld (accessed on April 20, 2022). https://mathworld.wolfram.com/ConfluentHypergeometricFunctionoftheFirstKind.html.

[17] E. W. Weisstein. *"Spherical Harmonic."* Mathworld (accessed on April 20, 2022). https://mathworld.wolfram.com/SphericalBesselFunctionoftheFirstKind.html

[18] L. Hamaide, C. McCabe. *"Fuelling the search for light dark matter-electron scattering"* October 6, 2021. doi:10.48550/arXiv.2110.02985.

[19] E. W. Weisstein. *"Gamma Function."* Mathworld (accessed on April 20, 2022). https://mathworld.wolfram.com/GammaFunction.html.

[20] D. E. Soper. *Galilean boost symmetry* 4 April, 2011. https://pages.uoregon.edu/soper/QuantumMechanics/boosts.p

[21] D, J. Griffiths, D. F. Schroeter. *"Introduction to Quantum Mechanics"* August, 2018.

[22] M. Wong, M. Vlietstra. *"Electron binding energy."* Radiopaedia.org. (accessed on April 20 2022). https://doi.org/10.53347/rID-67683

[23] E. W. Weisstein. *"Spherical Bessel Function of the First kind."* Mathworld (accessed on April 20, 2022). https://mathworld.wolfram.com/SphericalBesselFunctionoftheFirstKind.html

[24] E. W. Weisstein. *"Wigner 3j-Symbol."* Mathworld (accessed on April 20, 2022). https://mathworld.wolfram.com/Wigner3j-Symbol.html

[25] T. W. Ruijgrok, B. R. A. Nijboer. *"Recoil-induced excitation of atoms by neutron scattering"* Physica A, July 1983. doi:10.1016/0378-4371(83)90065-1